Available online at www.sciencedirect.com
SCIENCE DIRECT
Biochemical Pharmacology 69 (2005) 1533–1541
Biochemical Pharmacology
www.elsevier.com/locate/biochempharm

# Electrochemical characterisation of the human cytochrome P450 CYP2C9

D.L. Johnson [a], B.C. Lewis [b], D.J. Elliot [b], J.O. Miners [b], L.L. Martin [a,*]

[a] *School of Chemistry, Monash University, Vic. 3800, Australia*
[b] *Department of Clinical Pharmacology, Flinders Medical Centre and Flinders University School of Medicine, SA 5042, Australia*

Received 2 December 2004; accepted 21 February 2005

**Abstract**

The electrochemistry of human cytochrome P4502C9 (CYP2C9) was characterised using purified His-tagged enzyme. The His-tagged enzyme was shown to have similar functional characteristics to native CYP2C9 heterologously expressed in *Escherichia coli* and to the CYP2C9 activity of human liver microsomes. Evidence was observed for a reversible one-electron transfer between the P450 heme and the electrode. Both pH and ionic strength influenced the electrochemical behaviour of CYP2C9. A range of substrates was investigated to determine the effect of the heme–substrate interaction on CYP2C9 redox potential. In the absence of oxygen, tolbutamide, diclofenac, warfarin and sulfaphenazole did not alter the redox potential of the iron heme. In contrast, torsemide, carbon monoxide and oxygen led to an anodic shift in redox potential. These results suggest alternative mechanisms by which CYP2C9 (and by inference other P450 enzymes) may alter redox potential to facilitate electron delivery from physiological donors.


*Keywords:* Cytochrome P450; CYP2C9; Electrochemistry; Substrate shift; Midpoint potential; DDAB

## 1. Introduction

The cytochromes P450 are a superfamily of hemoproteins primarily involved in the oxidative biotransformation of hydrophobic substrates [1]. Apart from metabolising a myriad of xenobiotics (drugs, environmental pollutants, dietary chemicals), P450 enzymes also contribute to the biosynthesis and catabolism of endogenous compounds throughout many species [2].

The redox characteristics of P450 enzymes are of considerable interest, evidenced by extensive, ongoing studies over the past 30 years [3]. Perhaps the most interesting observation has been that the redox potential of P450 enzymes in solution are generally below that of the physiological electron donor [4,5]. Thus, the electronic structure of the iron heme at the active site of P450 enzymes must undergo a fundamental change prior to electron transfer from adrenodoxin in mitochondria or cytochrome P450 oxidoreductase (OxR) in microsomes [2]. This is thought to occur through a conformational change in protein structure or a significant change in electronic environment at the active site [2]. It is widely accepted that binding of substrates to the ferric P450 enzyme induces a change in spin state, from low spin to high spin [5–8]. Until recently, it has also been widely accepted that this change in spin state leads to an anodic shift in redox potential, from below to above the donor redox potential, allowing thermodynamically favourable electron transfer [5]. Indeed, this relationship has been verified for a number of different P450 enzymes in solution, including $P450_{cam}$ (CYP101, [6]), $P450_{BM3}$ (CYP102, [9]) and $P450_{scc}$ (CYP11A1, [8]). However, more recently, we [10] and others [11,12] have reported that under certain conditions, many P450 enzymes do not demonstrate this substrate-induced shift in redox potential. When P450 enzymes are immobilised at electrodes designed to mimic a biological membrane, and probed by direct electrochemical methods, P450 redox potentials are significantly higher than those reported in solution [2]. Furthermore, anodic shifts of ~50 mV have been observed for CYP102 [11] and $P450_{c17}$ (CYP17) [10] and $P450_{3A4}$ (CYP3A4) [13] in the presence of oxygen, a crucial component of P450 reactions. Elucidation of P450 mechanism has also been hindered by inconsistent reports for the same enzyme. For example

*Abbreviations:* CYP, cytochrome P450; CYP2C9, cytochrome P4502C9; DDAB, didodecyldimethylammonium bromide; $E_{mid}$, midpoint potential; $\Delta E$, peak separation; $I$, ionic strength; $i_{pc}/i_{pa}$, cathodic peak current divided by anodic peak current; $k_s$, electron transfer rate constant; NHE, Normal Hydrogen Electrode; OxR, cytochrome P450 oxidoreductase; PGE, edge-oriented pyrolytic graphite

* Corresponding author. Tel.: +61 3 9905 4514; fax: +61 3 9905 4597.
*E-mail address:* Lisa.Martin@sci.monash.edu.au (L.L. Martin).

0006-2952/$ – see front matter © 2005 Elsevier Inc. All rights reserved.
doi:10.1016/j.bcp.2005.02.020

over 20 individual reports have been published on the redox properties of CYP101 revealing a wide range of redox potentials and an inconclusive substrate effect [20].

CYP2C9 is recognised as one of the most important drug-metabolising enzymes in humans [14] responsible for the hepatic clearance of *S*-warfarin, phenytoin, tolbutamide, torsemide and many non-steroidal anti-inflammatory agents [14]. Despite being an enzyme of widespread pharmacological and toxicological interest, CYP2C9 is a largely uncharacterised enzyme for which the molecular basis of drug recognition remains unclear. Although six substrate recognition sites have been identified on CYP2C9 [14–18], the redox thermodynamics and kinetics remain conspicuously absent in the literature. A CYP2C9 X-ray crystal structure has been recently reported, with and without the substrate *S*-warfarin in the active site [19]. The structures identified a large substrate-binding pocket with sufficient volume to accommodate at least two substrate molecules. Interestingly, the X-ray structures found that the substrate is bound some distance from the catalytic site, suggesting that a significant conformational rearrangement is required prior to a catalytic reaction. Historically, all bacterial and mammalian P450s were believed to act in a similar manner, reflected in the use of CYP101 as a ''model'' P450 enzyme, despite sequence homologies as low as 30% [2]. In contrast, the CYP2C family comprising 2C8, 2C9, 2C18 and 2C19 have >82% sequence homology, allowing direct comparison between isoforms [14].

In this study, we report a purification procedure for catalytically competent CYP2C9, present the hitherto unreported redox behaviour of CYP2C9 and examine the heme–substrate interaction of this enzyme. The environment of a biological membrane was mimicked for all electrochemical experiments, since a lipid environment has been shown to affect P450 conformation is often a fundamental requirement of efficient P450 activity [20–27] and hydrophobic interactions have been implicated in P450 donor–acceptor electron transfer complexes [28].

## 2. Materials and methods

### 2.1. Materials

All chemicals were analytical reagent grade and used without further purification. Milli-Q water was used both as a solvent and in all washing steps. Phosphate buffered solutions (pH range 5.8–8.2) were used throughout this work, unless otherwise indicated. Restriction enzymes were purchased from New England Biolabs Inc. (Beverly, MA, USA). Diclofenac, sulfaphenazole, tolbutamide and 3-[(3-cholamidopropyl)dimethylamino]-1-propanesulfonate (CHAPS) were purchased from Sigma–Aldrich (Sydney, Australia), and 4′-hydroxydiclofenac was purchased from BD Gentest (Woburn, MA, USA). Torsemide (1-isopropyl-3-[(3-hydroxymethylanilino)-3-pyridyl]-sulfonylurea) and methylhydroxymethyltorsemide (1-isopropyl-3-[(4-m-(hydroxytoluidino)-3-pyridyl)sufonyl]urea) were supplied by Boehringer Mannheim International (Mannheim, Germany). *S*-Warfarin was a kind gift from Professor W.F. Trager (University of Washington, Seattle, WA, USA). *Escherichia coli* DH5α cells were purchased from Life Technologies (Melbourne, Australia). Anti-human CYP2C9 IgG was purchased from Research Diagnostics Inc. (Flanders, NJ, USA) and was used in parallel with the QIAexpress Tetra-His Antibody (Qiagen Australia, Doncaster, Australia). Gel purified oligonucleotides were supplied by Sigma–Genosys (Sydney, Australia), and Shrimp Alkaline Phosphatase by Roche Diagnostics GmbH (Penzberg, Germany). Nickel-nitrilotriacetic acid agarose (Ni-NTA) was obtained from Qiagen. All other chemicals and reagents were purchased from Sigma–Aldrich (Sydney, Australia) unless otherwise stated.

### 2.2. CYP2C9 and oxidoreductase cDNAs

N-Terminus modifications previously shown to promote high levels of bacterial expression of human P450s were made to the wild-type CYP2C9 cDNA, as previously documented [29]. The CYP2C9 cDNA was modified for bacterial expression by replacing the second codon with GCT (codes for Ala), deleting codons 3–20, and adjusting codons 21–26 for bacterial codon bias. To facilitate protein purification, a 6× histidine tag was added to the C-terminus of CYP2C9 using PCR, incorporating 3′ oligonucleotides containing the desired additions: forward primer, 5′-AGG ATC CAT CGA TGC TTA GGA GGT CAT ATG GCT CG-3′; reverse primer, 5′-T**GT CGA** CTT AGT GAT GGT GAT GGT GAT GAG ATC TGA CAG GAA TGA AGC A-3′. Generation of a *Sal*I restriction site (bold text) 3′ to the stop codon aided subsequent DNA manipulations. The 1476 bp PCR product was digested with *Nde*I and *Sal*I and ligated into the pCW ori(+) plasmid. pCW-CYP2C9 was transformed into DH5α *E. coli* cells and colonies screened for the correct plasmid by restriction enzyme analysis. Plasmid DNA was purified with the QIAprep Spin Miniprep Kit (Qiagen) and confirmed on both strands by sequencing (ABI Prism 3100). The cDNA coding for OxR consisted of the OmpA signal sequence fused upstream of the full-length native rat OxR (rOxR) sequence [29]. The rOxR expression construct was generated using the bacterial plasmid, pACYC.

### 2.3. Heterologous expression and purification of His-tagged CYP2C9

pCW-CYP2C9-His and pACYC-rOxR were transformed separately into DH5α *E. coli* cells. Cells were cultured and membrane fractions separated as described previously [29]. His-tagged CYP2C9 was purified by column chromatography using Ni-NTA Magnetic Agarose Beads (Qiagen). To avoid histidine contamination, imida-

zole (20 mM) was added to samples along with the equilibration buffer (SR Buffer: 10 mM $K_2HPO_4/KH_2PO_4$ buffer pH 7.6, 6 mM $Mg(OAc)_2$, 0.1 mM DTT, 20% glycerol, plus 0.5% CHAPS, 0.5 M KCl). Solubilised samples were directly applied to a pre-equilibrated column (10-bed volumes) and subsequently washed with 10-bed volumes of Wash Buffer (SR Buffer without $Mg(OAc)_2$). Protein was eluted in five-bed volumes of Wash Buffer containing 500 mM imidazole. Eluates were monitored at 420 (presence of $Fe^{3+}$) and 660 nm (total protein) prior to detection by Western blotting. CYP2C9 fractions were pooled and dialyzed overnight in two changes of CHAPS-free buffer (1 M $K_2HPO_4/KH_2PO_4$ pH 7.6, 10% glycerol, 0.1 mM DTT, 1 mM EDTA). Total protein and P450 concentrations were measured spectroscopically [30,31].

### 2.4. Western blot analysis

Equal amounts of total protein from each fraction (1 μg) were subjected separately to SDS-PAGE [32]. Proteins were rectilinearly transferred onto nitrocellulose (0.45 μm) and probed with either: (i) anti-human CYP2C9 primary antiserum (1:2000 dilution) and goat anti-rabbit IgG (1:2000 dilution; H+L-HRP) as the secondary antibody (Southern Biotechnology Associates Inc., Birmingham, USA) with human liver microsomes (10 μg) as a positive control, or (ii) with anti-His antiserum (HRP-conjugated; 1:2000 dilution) using human liver microsomes (10 μg) as a negative control and the 6× His Protein Ladder (Qiagen) as the positive control. Membrane-bound peptides conjugated with HRP were detected by chemiluminescence (Roche Diagnostics, Mannheim, Germany) and subsequently exposed to Omat autoradiographic film (Kodak).

### 2.5. Enzyme assays

Torsemide methylhydroxylase activity was measured according to the HPLC procedure of Miners et al. [33]. Briefly, incubation mixtures in a total volume of 0.5 ml contained purified CYP2C9 (5 pmol), rOxR (25 pmol), NADPH-generating system (1 mM NADP, 10 mM glucose 6-phosphate and 1 IU glucose 6-phosphate dehydrogenase) and torsemide (1–100 μM) in phosphate buffer (0.1 M, pH 7.4). Following a 5 min preincubation at 37 °C, reactions were initiated by the addition of NADPH generating system and continued for 15 min. Incubations were terminated by the addition of perchloric acid (0.05 ml, 11.6 M) and cooling on ice. After addition of the assay internal standard (4-methylumbelliferone, 2 nmol), the mixture was saturated with ammonium sulfate (0.75 g) and extracted with dichloromethane/propan-2-ol (85:15, 2 × 2 ml). The organic extract was dried under a stream of $N_{2\ (g)}$. Residues were reconstituted in the HPLC mobile phase (0.2 ml) and an aliquot (0.05 ml) injected on to a Waters Nova-pak C18 column (15 cm × 3.9 mm i.d., 4 μm particle size) which was eluted with 10 mM acetate buffer (pH 4.3)/acetonitrile (86.5:13.5) at a flow rate of 2 ml $min^{-1}$. Peaks were monitored by ultraviolet detection at 290 nm. Retention times for methylhydroxytorsemide and 4-methylumbelliferone were 2.35 and 6.04 min, respectively. Unknown concentrations were determined by reference to a standard curve constructed in the concentration range 0.1–2.5 μM. The lower limit of quantification was 0.025 μM. Under the reaction conditions employed, rates of torsemide methylhydroxylation were linear with respect to both incubation time and P450 concentration (respective linear ranges 5–75 min and 0.5–10 pmol CYP). Overall assay within day imprecision, determined from measurement of metabolite formation in eight separate incubations, was 4.2 and 2.9% at substrate concentrations of 5 and 25 μM, respectively. Inter-day variability, assessed from the slopes of 18 calibration curves, was 3.3%.

Incubations (0.5 ml) for the measurement of diclofenac 4′-hydroxylation activity contained purified CYP2C9 (1.5 pmol), rOxR (7.5 pmol), diclofenac (1–40 μM), and NADPH-generating system in phosphate buffer (0.1 M, pH 7.4). Reactions were carried out in air at 37 °C in a shaking water bath, and terminated after 20 min by the addition of perchloric acid (0.05 ml, 11.6 M) and cooling on ice. Following addition of ketoprofen (0.625 nmol, the assay internal standard), mixtures were vortex mixed and centrifuged at 5000 × *g* for 10 min. An aliquot (50 ul) of the supernatant fraction was injected onto a Waters Novapak C18 column (150 mm × 3.9 mm, 4 μm) at 25 °C and eluted with phosphate buffer (pH 7.4, 25 mM)/triethylamine/acetonitrile (80:0.016:20) at a flow rate of 1.5 ml $min^{-1}$. A stepped increase in acetonitrile (to 60%) between 8.5 and 10.5 min was used to elute diclofenac from the column. Analytes were detected by UV absorption at 270 nm. The retention times for 4′-hydroxydiclofenac and ketoprofen were 3.6 and 4.9 min, respectively. Unknown concentrations were determined from standard curves constructed for 4′-hydroxydiclofenac in the concentration range 0.1–2.5 μM. The lower limit of quantification was 0.025 μM. Rates of diclofenac 4′-hydroxylation were linear with respect to both incubation time and P450 concentration for the reaction conditions employed (respective linear ranges 10–40 min and 0.5–5 pmol CYP). Overall assay within day precision, determined from measurement of metabolite formation in six separate incubations, was 10.0 and 4.2% at substrate concentrations of 1 and 25 μM, respectively. Inter-day variability, assessed from the slopes of 13 calibration curves, was 4.9%.

### 2.6. Enzyme kinetics

Rates of methylhydroxytorsemide and 4′-hydroxydiclofenac formation versus substrate concentration were model-fitted using EnzFitter (Biosoft, Cambridge). In both

cases, kinetic data were best described by the single enzyme Michaelis–Menten equation.

### 2.7. Electrochemical characterisation

Unless otherwise noted, electrochemical experiments were conducted in a nitrogen-filled glove box in order to alleviate complications associated with oxygen catalysis and subsequent peroxide formation. Cyclic voltammograms were recorded at least four times with separate buffer and different electrodes using a Bioanalytical Systems (BAS) Model 100B electrochemical analyser. Scan rates varied between 5 and 1500 mV $s^{-1}$. Voltammetric data were obtained using an edge-oriented pyrolytic graphite (PGE) electrode (built in-house), radius 2.0 mm. Before each experiment, the electrode surface was polished with an alumina/water slurry (alumina particle size 1 μm, followed by 0.3 μm), washed and sonicated for 1 min to remove adsorbed alumina. The reference and counter electrodes were Ag/AgCl (3 M KCl, BAS) and platinum wire, respectively. The reference electrode was regularly calibrated against the $[Fe(CN)e]^{3-/4-}$ couple in 1 M $KNO_3$. All potentials are quoted versus NHE. Midpoint (reduction) potentials ($E_{mid}$) were calculated as the average of the oxidation ($E_{pa}$) and reduction ($E_{pc}$) peaks, the peak separation ($\Delta E$) was calculated as the difference between $E_{pc}$ and $E_{pa}$, and the peak current ratio ($i_{pc}/i_{pa}$) was calculated by dividing the cathodic peak current ($i_{pc}$) by the anodic peak current ($i_{pa}$).

Typically, a solution of didodecyldimethylammonium bromide (DDAB) was applied to the clean electrode surface (3 μl of a 0.1 M stock in chloroform or ethanol) and allowed to dry. CYP2C9 (2.65 ng; 0.047 pmol) was then added to the surface and left for 2 min before immersing in the buffered solution at the required pH. Data were collected using four separate electrodes, and the buffer was replaced regularly at each pH to avoid artifacts. 1.0 and 0.1 M phosphate buffers were used throughout as indicated.

Substrate/inhibitor binding was evaluated in three different ways at a variety of concentrations as described elsewhere [10]. Saturating the buffer with $CO_{(g)}$ prior to addition of the electrode and allowing 5 min for equilibration assessed binding of CO to the heme iron.

## 3. Results

### 3.1. Expression and kinetic characterisation of CYP2C9

*E. coli* transformed with the modified CYP2C9 cDNA expressed high levels of His-tagged CYP2C9 (average 320 nmol P450 per litre of culture). The CYP2C9 concentration of solubilised membrane fractions was 623 nmol P450 per litre of culture. SDS-PAGE of His-tagged CYP2C9 yielded a single band of approximately 56 kDa

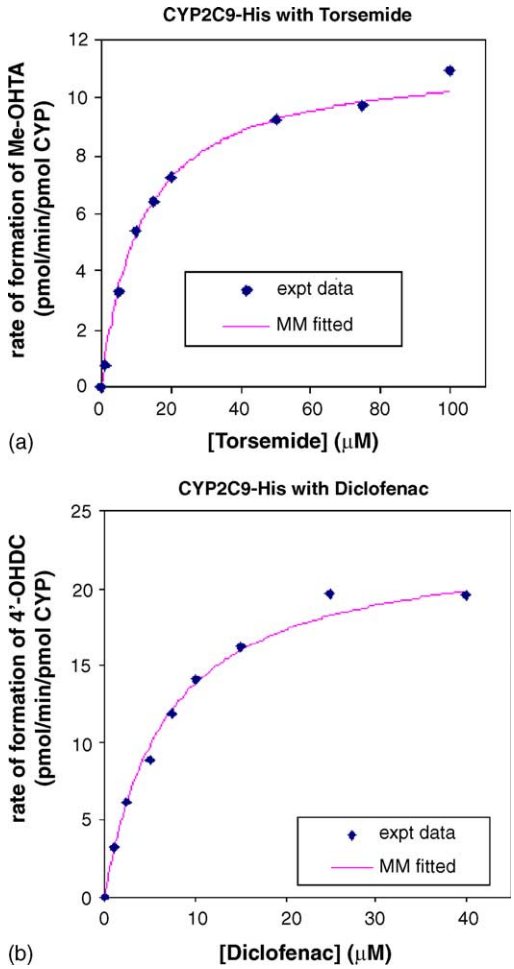


Fig. 1. Kinetic plots of His-tagged CYP2C9 with (a) torsemide and (b) diclofenac as substrates. Rates of hydroxymethyltorsemide and 4′-hydroxydiclofenac formation vs. substrate concentration were model-fitted using EnzFitter (Biosoft) to the single enzyme Michaelis–Menten equation. Points represent the mean of duplicate estimates, while curves are from model-fitting.

with both the anti-CYP2C9 and anti-His antibodies (results not shown). The purified His-tagged CYP2C9 exhibited torsemide methylhydroxylase and diclofenac 4′-hydroxylase activity when reconstituted with membrane-bound rOxR. Both reactions followed Michaelis–Menten kinetics (Fig. 1). The respective derived apparent $K_m$ and $V_{max}$ values (± parameter S.E. of fit) for torsemide methylhydroxylation and diclofenac 4′-hydroxylation were $11.4 \pm 0.1$ and $6.8 \pm 0.01$ μM, and $11.5 \pm 0.5$ and $23.2 \pm 0.01$ pmol/min/pmol P450.

### 3.2. Electrochemistry of CYP2C9

A PGE electrode was sequentially modified with films of didodecyldimethylammonium bromide (DDAB) and the bacterially expressed CYP2C9. No redox response was observed in the absence of CYP2C9. Reversible voltammograms with well-defined peak shapes were obtained for CYP2C9 confined at the electrode surface, consistent with electron exchange between the electrode and the heme. The cyclic voltammogram differed slightly throughout

initial cycles until the surface had reorganised into an optimal structure, after which reproducible data could be obtained for several hours indicating a stable, compact film. These findings confirmed independent results from our laboratory with CYP17 [10], demonstrating that surface reorganisation does not influence the thermodynamic or kinetic parameters $E_{mid}$, $\Delta E$, $k_s$ and $i_{pc}/i_{pa}$.

A representative series of sequential voltammograms under anaerobic conditions are shown in Fig. 2a. Fig. 2b highlights a linear relationship between the scan rate ($v$) and peak current ($i_p$), indicative of an immobilised redox-active species with little or no influence of protein diffusion away from or to the electrode surface. At pH 7.4, the redox response was centered on −41 mV, consistent with that expected for a ferric/ferrous redox couple. Although both reductive and oxidative redox processes revealed symmetric peaks, the area under the reductive peak was either the same or slightly larger than the area under the oxidative peak, similar to that noted previously for CYP17 [10].

The reduction potential of CYP2C9 was influenced by both the pH and the ionic strength ($I$) of the buffer. Variation of pH led to a shift in $E_{mid}$ of between −52 and −55 mV per pH unit, close to the theoretical value of −59 mV per pH unit predicted for the coupling of a single proton transfer to the electron transfer event. This trend was consistent between the pH limits 5.8 and 8.0 in the presence and absence of substrate, indicating that the p$K_a$ associated with the pH dependence lies well outside physiological pH (Fig. 3). Variation of $I$ from 0.1 to 1 M resulted in an anodic shift in $E_{mid}$. This effect was greater at lower pH (∼22 mV at pH 5.8) than at high pH (∼9 mV at pH 8.0). Higher $I$ effectively stabilises the ferrous heme form over the ferric heme form.

The electron transfer rate constant ($k_s$), determined by the method of Laviron [34], varied significantly with pH. The general trend was for faster $k_s$ at higher pH, calculated to be 139 $s^{-1}$ at pH 6.0, 150 $s^{-1}$ at pH 7.4 and 165 $s^{-1}$ at pH 8.2. These $k_s$ values are measured in the absence of oxygen, and simply indicate the efficacy of electrode–

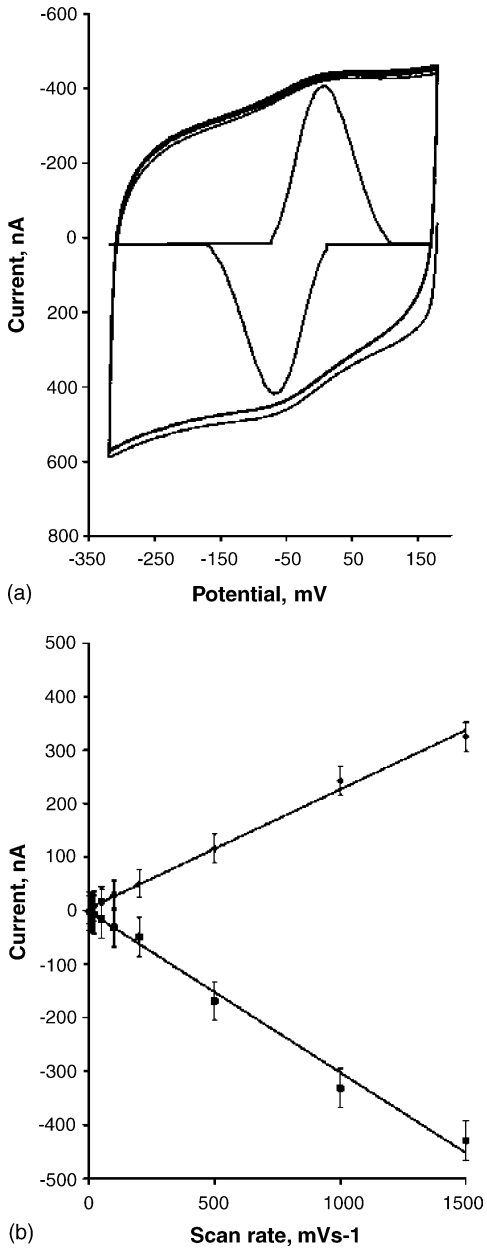


Fig. 2. (a) Typical cyclic voltammograms of human CYP2C9 obtained at a DDAB-modified PGE electrode in the absence of oxygen. The stability of the film is highlighted, with scans taken at hourly intervals after first putting the electrode into buffer. Sequential scans are overlaid. Inset is a voltammogram with capacitive current subtracted, $v = 50$ mV $s^{-1}$. (b) Variation of peak current ($i_p$) with scan rate ($v$) for CYP2C9. The linear relationship indicates mass transport plays an insignificant role in electrode dynamics. Buffer is 0.1 M potassium phosphate, pH 7.4.

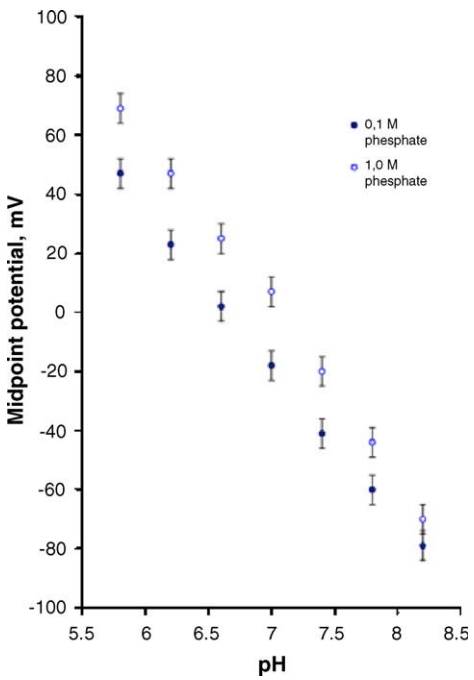


Fig. 3. The influence of pH and ionic strength ($I$) on midpoint potentials ($E_{mid}$) of purified CYP2C9 adsorbed at a DDAB-modified PGE electrode. The slopes of each plot are 0.1 M (filled circles) = 52.4 mV $pH^{-1}$ and 1.0 M (open circles) = 57.5 mV $pH^{-1}$.

Table 1
Substrate (s)- and inhibitor (i)-induced shifts in $E_{mid}$ observed for CYP2C9 immobilised at a DDAB-modified PGE electrode

| Substrate/inhibitor of CYP2C9 | $K_m$ (μM) | $K_i$ (μM) | CYP2C9 (mV) | $E_{mid}$ CYP2C9 + substrate (mV) | Substrate shift (mV) |
|---|---|---|---|---|---|
| Torsemide (s) | 11.4 | | −41 | −19 | 22 |
| Diclofenac (s) | 6.8 | | −41 | −41 | 0 |
| Tolbutamide (s) | 120[a] | | −41 | −37 | 4 |
| *S*-Warfarin (s) | 6[b] | | −41 | −36 | 5 |
| Sulfaphenazole (i) | | 0.1[c] | −41 | −41 | 0 |
| $CO_{(g)}$ | | | −41 | 8 | 49 |

Experimental conditions were 0.1 M phosphate buffer, pH 7.4; $v = 50$ mV $s^{-1}$.
[a] Tolbutamide $K_m$ value taken from [37].
[b] *S*-Warfarin $K_m$ taken from [36].
[c] Sulfaphenazole $K_i$ taken from [35].

protein electron exchange, not the efficacy under turnover conditions.

### 3.3. Redox characterisation of CYP2C9 substrates and inhibitors

Voltammetric experiments were undertaken to ascertain the effect of heme–substrate and heme–inhibitor interactions on the redox properties of CYP2C9, using the substrates tolbutamide, torsemide, diclofenac and *S*-warfarin, along with the inhibitor sulfaphenazole. The CYP2C9 $K_i$ or $K_m$ values for these compounds encompass three orders of magnitude: sulfaphenazole, 0.1 μM [35]; *S*-warfarin, 6 μM [36]; diclofenac, 6.8 μM (this work); torsemide, 11.4 μM (this work); and tolbutamide, 120 μM [37]. In addition, we examined the redox properties of the CYP2C9 heme in the presence of $CO_{(g)}$. Table 1 displays the results of these experiments, and Fig. 4 shows representative voltammograms before (dashed line) and after (solid line) addition of $CO_{(g)}$.

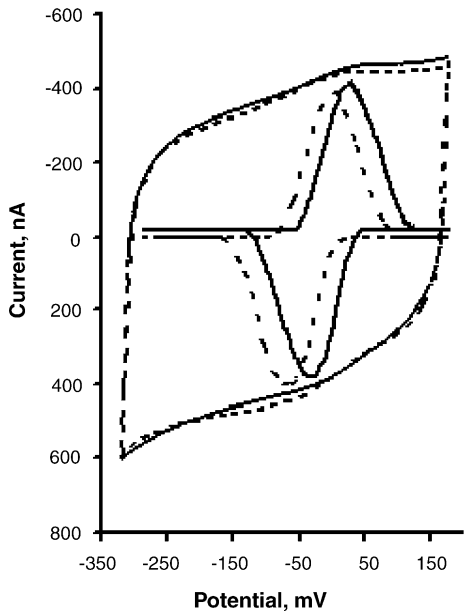


Fig. 4. Cyclic voltammograms of CYP2C9 immobilised at a DDAB-modified PGE electrode before (dashed line) and after (solid line) bubbling $CO_{(g)}$ through the buffer. Inset are the corresponding baseline-subtracted voltammograms. Buffer is 0.1 M potassium phosphate, pH 7.4. Scan rate, 50 mV $s^{-1}$.

The redox properties of CYP2C9 were significantly different in the presence of oxygen. Cyclic voltammograms in aerated buffer induced an anodic shift (∼50 mV) and a dramatic increase in cathodic current. However, this response was unstable and led to a total loss in faradaic current after 5–10 cycles, an effect we attribute to peroxide formation and consequent protein denaturation.

## 4. Discussion

His-tagged CYP2C9, an enzyme of major importance in human drug metabolism [14], was expressed in *E. coli* and purified. When reconstituted with rOxR, the His-tagged CYP2C9 exhibited similar kinetic characteristics to native CYP2C9 and human liver microsomal CYP2C9 with the prototypic substrates torsemide and diclofenac. The apparent $K_m$ for torsemide methylhydroxylation by His-tagged CYP2C9 observed here (viz. 11.5 μM) is close in value for the reaction catalysed by native CYP2C9 expressed in *E. coli* (11.9–20.2 μM) [29] and by human liver microsomes (11.2 μM) [33]. Similarly, the apparent $K_m$ for diclofenac 4′-hydroxylation by His-tagged CYP2C9 (6.8 μM) is similar to values reported for the native enzyme expressed in *E. coli* (3.6–8.1 μM) [18,38] and by human liver microsomes (9 μM) [39]. In addition, the $V_{max}$ values (equivalent to $k_{cat}$) for torsemide methylhydroxylation and diclofenac 4′-hydroxylation by the His-tagged and native CYP2C9 expressed in *E. coli* were also close in value (11.5 versus 8.6 and 23.2 versus 17.1 pmol/min/pmol P450, respectively) [29](D.J. Elliot and J.O. Miners, unpublished data). Domanski et al. [40] have previously reported similar results for His-tagged CYP3 A4, where activity did not differ from that of the wild-type protein. These data indicate that the C-terminal histidine tag does not affect substrate binding and turnover, and hence presumably does not significantly alter the conformation of the CYP2C9 active site.

The purified CYP2C9 was immobilised at a pyrolytic graphite electrode modified with the surfactant DDAB, a molecule capable of both electrostatically interacting with

the negatively charged PGE surface and mimicking a lipid-like environment for interaction with the P450 [41]. Rapid electronic communication was observed between immobilised CYP2C9 and the electrode surface ($k_s$ ~150 $s^{-1}$), an order of magnitude greater than that identified as the lower limit for use as a bioelectrocatalyst [42,43]. Several of the observed electrochemical parameters and trends including $\Delta E$, $\omega^{1/2}$ (peak-width at half-height), electroactive surface coverage, and the influence of pH on $E_{mid}$ are similar to those previously reported for CYP17 [10].

Substrate binding to many cytochromes P450 studied to date results in a change in the spin state of the $Fe^{3+}$ heme, from low spin to high spin [5–8]. This has often correlated to an anodic shift in $E_{mid}$, facilitating the transfer of electrons from the donor [5]. The well-characterised CYP101 has a solution redox potential below that of the natural electron donor putidaredoxin (−306 and −228 mV, respectively [44,45]). Binding of camphor raises the redox potential around 130 mV, enough to allow natural electron flow [6]. Thus, substrate binding is widely believed to act as a thermodynamic trigger preceding the electron transfer event [5]. In this study, the electrochemical parameters of CYP2C9 were evaluated in the presence of a range of different substrates and an inhibitor (Table 1). The substrate/inhibitor $K_m$ or $K_i$ values ranged from 0.1 (sulfaphenazole, [35]) to 120 μM (tolbutamide, [37]). The basic voltammetric parameters ($E_{mid}$, $\Delta E$, $k_s$, $i_{pc}/i_{pa}$) were virtually unchanged for tolbutamide, diclofenac, *S*-warfarin and sulfaphenazole over a wide range of experimental conditions. This suggests that in the absence of oxygen, these substrates bind some distance from the heme, thus having a negligible effect on the electronic environment about the iron atom. In contrast, torsemide, a compound with a relatively low $K_m$ (11.4 μM), which shares structural similarities with tolbutamide ($K_m$ 120 μM), induced a small anodic shift in $E_{mid}$. The origin of this shift remains unclear and cannot be rationalised simply by structure or the presence of functional groups. Interestingly, a solution saturated with either $CO_{(g)}$ or $O_{2\ (g)}$ induced an anodic shift of ~50 mV (Fig. 4), confirming that the observed redox signal resulted from the heme iron and that small molecules can access the active site of immobilised CYP2C9. A previous electrochemical study of CYP101 found that although substrates did not influence the redox potential, catalytic activity could be achieved in the presence of oxygen [43]. Although CYP2C9 redox behaviour is minimally influenced by substrate in the absence of oxygen (the substrate appears to dock some distance from the catalytic site [19]) it may indicate that binding of oxygen initiates a geometric and electronic rearrangement that brings the substrate closer to the heme and allows for catalytic activity. Indeed, the anodic potential shift in the presence of oxygen has been recently identified as a means by which the P450 $E_{mid}$ may rise, in the presence or absence of standard substrates, to facilitate a thermodynamically favourable electron transfer event [46].

The $E_{mid}$ values observed for CYP2C9 are well above those reported for most P450 enzymes in solution [10]. At pH 7.4 and $I = 0.1$ M, the observed $E_{mid}$ was −41 mV, whereas potentiometric values reported for cytochromes P450 in solution are typically between −400 and −280 mV [10]. Similar anomalies have been identified for CYP101 (−303 in solution [6,44,45], −139 when immobilised at a clay-modified electrode [47]), CYP102 (−368 in solution [9], approximately −30 mV at a lipid-modified electrode [11]), CYP11A1 (−412 in solution [8], approximately −37 immobilised at an unmodified electrode [48]) and others, including P450cin (CYP176A) and CYP3A4. These data highlight the influence of experimental conditions; solution studies are often undertaken in a hydrophilic, aqueous environment, whereas studies using immobilised protein are often in the presence of lipid-like compounds that trap the enzyme in a hydrophobic layer. This simple experimental modification has led to shifts in redox potential of up to 400 mV relative to solution experiments [10]. Perhaps the most significant point is that the presence of surfactant changes the P450 $E_{mid}$ to a value above that of the electron transfer donor, thus enhancing the thermodynamics of electron transfer. (The [2Fe-2S]-containing ferredoxin in mitochondrial and bacterial electron delivery pathways has an $E_{mid}$ approximately −250 mV [49] and the FMN prosthetic in ferredoxin reductase for microsomal pathways has an $E_{mid}$ approximately −192 mV [9]). Accordingly, the argument for a substrate-induced shift in redox potential may only relate to isolated P450 (i.e., P450 outside a biological membrane or lipid-like environment). Thus, without any other contributing factors like substrate or even oxygen, a lipid environment may be able to alter the electron transfer event from a thermodynamically unfavourable process (positive $\Delta G$) to a favourable, spontaneous process (negative $\Delta G$). This point is further emphasised by the fact that a lipid-like environment is required for catalytic activity [12,50–52] and numerous other structural and electronic properties [20–27] for many P450 enzymes.

## 5. Conclusions

We have expressed and purified CYP2C9, and characterised the enzyme by direct electrochemistry. Rapid electron transfer was observed between a modified pyrolytic graphite electrode and the heme active site for immobilised CYP2C9. The heme redox potential (−41 mV) is at the higher end of the range reported for P450 enzymes, and is above that of the physiological electron donor cytochrome P450 oxidoreductase. The redox potential was influenced by both pH and ionic strength, consistent with the redox behaviour reported for other P450 enzymes. Interestingly, of a range of CYP2C9 substrates evaluated, only torsemide (22 mV), carbon monoxide (49 mV) and oxygen (~50 mV) induced a significant shift in redox potential.

## Acknowledgements

The authors would like to acknowledge funding from a program grant awarded by Flinders University Institute for Research in Science and Technology and development and project grants from the National Health and Medical Research Council of Australia Grant (No. 284421 and 275536).

## References

[1] Guengerich FP. Common and uncommon cytochrome P450 reactions related to metabolism and chemical toxicity. Chem Res Toxicity 2001;14:611–50.
[2] Li H. In: Messerschmidt A, Huber R, Wieghardt K, Poulos T, editors. Cytochrome P450 in Handbook of Metalloproteins. Chichester: John Wiley and Sons; 2001. p. 267–82.
[3] Omura T. Forty years of cytochrome P450. Biochem Biophys Res Commun 1999;266:690–8.
[4] Hanukoglu I. Electron transfer proteins of cytochrome P450 systems. Adv Mol Cell Biol 1996;14:29–55.
[5] Sligar SG. Coupling of spin, substrate, and redox equilibria in cytochrome P450. Biochemistry 1976;15:5399–406.
[6] Sligar SG, Gunsalas IC. A thermodynamic model of regulation: modulation of redox equilibria in camphor monoxygenase. Proc Natl Acad Sci USA 1976;73:1078–82.
[7] Fisher MT, Sligar SG. Control of heme protein redox potential and reduction rate: linear free energy relation between potential and ferric spin state equilibrium. J Am Chem Soc 1985;107:5018–9.
[8] Light DR, Orme-Johnson NR. Beef adrenal cortical cytochrome P450 which catalyzes the conversion of cholesterol to pregnenolone. J Biol Chem 1981;256:343–50.
[9] Daff SN, Chapman SK, Turner KL, Holt RA, Govindaraj S, Poulos TL, et al. Redox control of the catalytic cycle of flavocytochrome P450BM3. Biochemistry 1997;36:13816–23.
[10] Johnson DL, Ph.D. Thesis. Flinders University, Australia, 2004.
[11] Fleming BD, Tian Y, Bell SG, Wong L-L, Urlacher V, Hill HAO. Redox properties of cytochrome P450BM3 measured by direct methods. Eur J Biochem 2003;270:4082–8.
[12] Aguey-Zinsou K-F, Bernhardt PV, De Voss JJ, Slessor KE. Electrochemistry of P450cin: new insights into P450 electron transfer. J Chem Soc Chem Commun 2003;3:418–9.
[13] Estavillo C, Lu Z, Jansson I, Schenkman JB, Rusling JF. Epoxidation of styrene by human cyt P450 1A2 by thin film electrolysis and peroxide activation compared to solution reactions. Biophys Chem 2003;104:291–6.
[14] Miners JO, Birkett DJ. Cytochrome P450 2C9: an enzyme of major importance in human drug metabolism. Br J Clin Pharmacol 1998;45:525–38.
[15] Melet A, Assrir N, Jean P, Lopez-Garcia MP, Marques-Soares C, Jaouen M, et al. Substrate selectivity of human cytochrome P450 2C9: importance of residues 476 365 and 114 in recognition of diclofenac and sulfaphenazole and in mechanism-based inactivation by tienilic acid. Arch Biochem Biophys 2003;409:80–91.
[16] Poli-Scaife S, Attias R, Dansette PM, Mansuy D. The substrate binding site of human liver cytochrome P450 2C9: an NMR study. Biochemistry 1997;36:12672–82.
[17] Hutzler JM, Wienkers LC, Wahlstrom JL, Carlson TJ, Tracy TS. Activation of cytochrome P450 2C9-mediated metabolism: mechanistic evidence in support of kinetic observations. Arch Biochem Biophys 2003;410:16–24.
[18] Flanagan JU, McLaughlin LA, Paine MJI, Sutcliffe MJ, Roberts GCK, Wolf CR. Role of conserved Asp293 of cytochrome P450 2C9 in substrate recognition and catalytic activity. Biochem J 2003;370:921–6.
[19] Williams PA, Cosme J, Ward A, Angove HC, Vinkovic DM, Jhoti H. Crystal structure of human cytochrome P450 2C9 with bound warfarin. Nature 2003;424:464–8.
[20] Djuricic D, Fleming BD, Hill HAO, Tian Y. In: Pombeiro AJL, Amatore C, editors. Trends in molecular electrochemistry. Marcel Dekker; 2004.
[21] Ruckpaul K, Rein H, Blanck J, Ristau O, Coon MJ. Molecular mechanisms of interactions between phospholipids and liver microsomal cytochrome P450LM2. Acta Biol Med German 1982;41:193–203.
[22] Omata Y, Aibara K, Ueno Y. Conformation between the substrate-binding site and heme of cytochrome P-450 studied by excitation energy transfer. Biochem Biophys 1987;912:115–23.
[23] Yun C-H, Ahn T, Guengerich FP. Conformational change and activation of cytochrome P450 2B1 induced by salt and phospholipid. Arch Biochem Biophys 1998;356:229–38.
[24] French JS, Guengerich FP, Coon MJ. Interactions of cytochrome P-450, NADPH-cytochrome P-450 reductase, phospholipid, and substrate in the reconstituted liver microsomal enzyme system. J Biol Chem 1980;255:4112–9.
[25] Miwa GT, Lu AYH. Studies on the stimulation of cytochrome P-450-dependent monooxygenase activity by dilauroylphosphatidylcholine. Arch Biochem Biophys 1981;211:454–8.
[26] Imaoka S, Imai Y, Shimada T, Funae Y. Role of phospholipids in reconstituted cytochrome P450 3 A form and mechanism of their activation of catalytic activity. Biochemistry 1992;31:6063–9.
[27] Voznesensky AI, Schenkman JB. Quantitative analyses of electrostatic interactions between NADPH-cytochrome P450 reductase and cytochrome P450 enzymes. J Biol Chem 1994;269:15724–31.
[28] Tamburini PP, Schenkman JB. Differences in the mechanism of functional interaction between NADPH-cytochrome P-450 reductase and its redox partners. Mol Pharmacol 1986;30:178–85.
[29] Boye SL, Kerdpin O, Elliot DJ, Miners JO, Kelly L, McKinnon RA, et al. Optimizing bacterial expression of catalytically active human cytochromes P450: comparison of CYP2C8 and CYP2C9. Xenobiotica 2004;34:49–60.
[30] Omura T, Sato R. The carbon monoxide-binding pigment of liver microsomes. J Biol Chem 1964;239:2379–85.
[31] Lowry OH, Rosebrough NJ, Farr AL, Randall RJ. Protein measurement with the folin phenol reagent. J Biol Chem 1951;193:267–75.
[32] Laemmli UK. Cleavage of structural proteins during the assembly of the head of bacteriophage T4. Nature 1970;227:680–5.
[33] Miners JO, Rees DLP, Valente L, Veronese ME, Birkett DJ. Human hepatic cytochrome P450 2C9 catalyses the rate-limiting pathway of torsemide metabolism. J Pharmacol Exp Ther 1995;272:1076–81.
[34] Laviron E. General expression of the linear potential sweep voltammogram in the case of diffusionless electrochemical system. J Electroanal Chem 1979;101:19–28.
[35] Miners JO, Smith KJ, Robson RA, McManus ME, Veronese ME, Birkett DJ. Tolbutamide hydroxylation by human liver microsomes. Kinetic characterisation and relationship to other cytochrome P450-dependent xenobiotic oxidations. Biochem Pharmacol 1988;37:1137–44.
[36] Haining RL. Enzymatic determinants of the substrate specificity of CYP2C9: role of B′-C loop residues in providing the pi-stacking anchor site for warfarin binding. Biochemistry 1999;38:3285–92.
[37] Miners JO, Birkett DJ. Use of tolbutamide as a substrate probe for human hepatic cytochrome P450 2C9. Methods Enzymol 1996;272:139–45.
[38] Ridderstrom M, Masimirembwa C, Trump-Kallmeyer S, Ahlefelt M, Otter C, Andersson TB. Arginines 97 and 108 in CYP2C9 are important determinants of the catalytic function. Biochem Biophys Res Commun 2000;270:983–7.
[39] Bort R, Mace K, Boobis A, Gomez-Lechon M-J, Pfeifer A, Castell J. Hepatic metabolism of diclofenac: role of human CYP in the minor oxidative pathways. Biochem Pharmacol 1999;58:787–96.

[40] Domanski TL, Liu J, Harlow GR, Halpert JR. Analysis of four residues within substrate recognition site 4 of human cytochrome P450 3A4: role in steroid hydroxylase activity and a-naphthoflavone stimulation. Arch Biochem Biophys 1998;350:223–32.
[41] Rusling JF. Enzyme bioelectrochemistry in cast biomembrane-like films. Acc Chem Res 1998;31:363–9.
[42] Joseph S, Rusling JF, Lvov YM, Friedberg T, Fuhr U. An amperometric biosensor with human CYP3 A4 as a novel drug screening tool. Biochem Pharmacol 2003;65:1817–26.
[43] Munge B, Estavillo C, Schenkman JB, Rusling JF. Optimization of electrochemical and peroxide-driven oxidation of styrene with ultrathin polyion films containing cytochrome P450cam and myoglobin. Chem Biochem 2003;4:82–9.
[44] Reipa V, Mayhew MP, Holden MJ, Vilker VJ. Redox control of the P450cam catalytic cycle: effects of Y96F active site mutation and binding of a non-natural substrate. J Chem Soc Chem Commun 2002;318–9.
[45] Wong LS, Vilkers VL. J Electroanal Chem 1995;389:201–3.
[46] Honeychurch MJ, Hill HAO, Wong L-L. The thermodynamics and kinetics of electron transfer in the cytochrome P450cam enzyme system. FEBS Lett 1999;451:351–3.
[47] Lei C, Wollenberger U, Jung C, Scheller FW. Clay-bridged electron transfer between cytochrome P450cam and electrode. Biochem Biophys Res Commun 2000;268:740–4.
[48] Nicolini C, Erokhin V, Ghisellini P, Paternolli C, Kumar Ram M, Sivozhelezov V. P450scc engineering and nanostructuring for cholesterol sensing. Langmuir 2001;17:3719–26.
[49] Johnson DL, Norman S, Tuckey RC, Martin LL. Electrochemical behaviour of human adrenodoxin on a pyrolytic graphite electrode. Bioelectrochemistry 2003;29:41–7.
[50] Hlavica P, Lewis DFV. Allosteric phenomena in cytochrome P450-catalyzed monoxygenations. Eur J Biochem 2001;268:4817–32.
[51] Ivanov YD, Kanaeva IP, Gnedenko OV, Pozdnev VF, Shumyantseva VV, Samenkova NF, et al. Optical biosensor investigation of interactions of biomembrane and water-soluble cytochromes P450 and their redox partners with covalently immobilized phosphatidylethanolamine layers. J Mol Recognit 2001;14:185–96.
[52] Zhang Z, Nassar A-EF, Lu Z, Schenkman J, Rusling JF. Direct electron injection from electrodes to cytochrome P450cam in biomembrane-like films. J Chem Soc Faraday Trans 1997;93:1769–74.